

Motion of hot spots in smoothed beams

L. Videau* and C. Rouyer

Commissariat à l'Energie Atomique, Centre d'Etudes de Limeil-Valenton, 94195 Villeneuve St. Georges Cedex, France

J. Garnier

Centre de Mathématiques Appliquées, Unité Mixte de Recherche 7641, Centre National de la Recherche Scientifique, Ecole Polytechnique, 91128 Palaiseau Cedex, France

A. Migus

Laboratoire pour l'Utilisation des Lasers Intenses, Unité Mixte de Recherche 7605, Centre National de la Recherche Scientifique and Commissariat à l'Energie Atomique, Ecole Polytechnique, 91128 Palaiseau Cedex, France

Received August 4, 1998; accepted March 8, 1999; revised manuscript received March 23, 1999

We develop a statistical model that describes the motion of a hot spot created by smoothing techniques. We define clearly the transverse and longitudinal instantaneous velocities of a hot spot and quantify its lifetime. This relevant parameter is found to be longer than the laser coherence time defined as the inverse of the spectrum bandwidth. We apply this model to the most usual smoothing techniques, using a sinusoidal phase modulation or a random spectrum. We give asymptotic results for hot spot velocities and lifetime for the cases of one-dimensional smoothing by spectral dispersion, smoothing by longitudinal spectral dispersion, and smoothing by optical fiber. © 1999 Optical Society of America [S0740-3232(99)02607-1]

OCIS codes: 030.6660, 030.6140, 140.3580.

1. INTRODUCTION

Smoothing techniques have been developed for the control of focal spot shape and hot spot distribution¹⁻³ in inertial confinement fusion applications. In the direct-drive scheme, optical smoothing helps to limit hydrodynamic instabilities by producing a time-integrated uniform focal spot. Long time contrast below 1% can be obtained with two-dimensional smoothing by spectral dispersion (2D-SSD) or smoothing by optical fiber (SOF).⁴⁻⁶ Nevertheless, the French Mégajoule Laser⁷ (LMJ) and the U.S. National Ignition Facility⁸ are designed for the indirect-drive scheme. The produced laser energy of 1.8 MJ is focused into a Hohlraum and irradiates the gold inner wall to be converted into x-rays. Up to now, static methods of smoothing such as by a kinoform phase plate⁹ were considered to be sufficient for indirect drive as opposed to direct drive, for which the underdense plasma creates parametric instabilities. These parametric instabilities—filamentation and Brillouin and Raman scattering¹⁰—are deleterious in that they may be responsible for energy losses as high as 30%. However, it was found that for indirect drive it is important to slow the wall expansion by using a gas inside the cavity and then adding a window to close the cavity. As a consequence, the laser beam also has to propagate through underdense plasma, as in the case of direct drive with the previously described parametric effects. Therefore it is important to reduce high intensities in space and in time for the LMJ National Ignition Facility configuration also. The shape of the focal spot can be optimized with a large circular or elliptical shape⁹ to limit the averaged intensity to a value

below 10^{15} W/cm², but the intensity is still too close to the instability threshold. Another proposed solution is to use two polarizations with two independent speckle patterns. This technique of polarization smoothing¹¹ decreases the fraction of intensities that are larger than the averaged intensity, the instantaneous contrast also being reduced, by a factor $1/\sqrt{2}$. A third solution would be to reduce the interaction time between hot spots (high laser intensities) and plasma. Smoothing techniques are relevant here in that they create inside the focal spot many hot spots that disappear rapidly within a few picoseconds. Although a low optical contrast is not required for indirect drive, it is necessary to turn off the hot spots in a short time. The use of one-dimensional techniques such as one-dimensional smoothing by spectral dispersion¹² (1D-SSD) or smoothing by longitudinal spectral dispersion (SLSD) is thus well adapted to this use. It is generally asserted that hot spots exist during a lifetime that corresponds to the laser coherence time, which is also the inverse of the spectral bandwidth.^{4,5} We shall see that this assumption is not correct for several smoothed beams.

In this paper we study more precisely the motion of the local maxima of the intensity distribution (the so-called hot spots), and we quantify the time decrease of the space-time correlation function for different optical smoothing techniques based on a temporal sinusoidal phase modulation. In Section 2 we present a statistical model that describes the electromagnetic field around the focal spot and the hot spot motion. In particular, we use Adler's theorem, which implies that the local shape of a hot spot is proportional to the generalized correlation

function defined in the space and time domains. In Section 3 we use the formalism for 1D-SSD, and Section 4 and Section 5 are devoted to SLSD and SOF, respectively.

2. RELEVANT STATISTICAL QUANTITIES FOR DESCRIBING THE HOT SPOT MOTION

In the following, the normalized complex electromagnetic field near the focal spot is denoted by $E(x, y, z, t)$, where x and y are the transverse spatial variables, z is the longitudinal one, and t is the time. We normalize the quantities so that the intensity $I(x, y, z, t)$ is simply equal to $|E(x, y, z, t)|^2$. We then may use Adler's theorem,^{13,14} which describes the local behavior of the intensity in the neighborhood of a local maximum centered at (X, Y, Z, T) :

$$I(X + x, Y + y, Z + z, T + t) = I(X, Y, Z, T)\Gamma(X, Y, Z, T, x, y, z, t). \quad (1)$$

Γ is the normalized four-dimensional correlation function (FCF) defined by

$$\Gamma(\mathbf{X}, T, \mathbf{x}, t) = \frac{\left| \left\langle E\left(\mathbf{X} + \frac{\mathbf{x}}{2}, T + \frac{t}{2}\right) E^*\left(\mathbf{X} - \frac{\mathbf{x}}{2}, T - \frac{t}{2}\right) \right\rangle \right|^2}{\left\langle I\left(\mathbf{X} + \frac{\mathbf{x}}{2}, T + \frac{t}{2}\right) \right\rangle \left\langle I\left(\mathbf{X} - \frac{\mathbf{x}}{2}, T - \frac{t}{2}\right) \right\rangle}, \quad (2)$$

where $\mathbf{X} = (X, Y, Z)$ and $\mathbf{x} = (x, y, z)$. This theorem is valid when $\Gamma(X, Y, Z, T, x, y, z, t) \gg I_0/I(X, Y, Z, T)$ ($I_0 = \langle |E_0(X, Y, Z, T)|^2 \rangle$). Here a statistical average is denoted by $\langle \cdot \rangle$. The capital letters correspond to the macroscopic variables, since (X, Y, Z, T) is the spatial/temporal reference point of the initial field. The lower-case letters (x, y, z, t) are related to microscopic variables, and we assume that the statistics of the field are locally stationary for these variables. For the maximum value of Γ , 1, the fields are identical, whereas the fields are totally incoherent for a null value. Using Eq. (1), we can determine the spatial/temporal shape of the intensity in the neighborhood of a maximum created at a given reference point (X, Y, Z, T) . In particular, we are interested in monitoring the time evolution of the spatial position of the maximum of the hot spot. We define the parametric plot $\{x(t), y(t), z(t)\}$ as the relative position of the maximum of intensity for each time t after ($t > 0$) or before ($t < 0$) the maximum is reached:

$$\Gamma(X, Y, Z, T, x(t), y(t), z(t), t) = \max_{x,y,z} [\Gamma(X, Y, Z, T, x, y, z, t)]. \quad (3)$$

We can define the instantaneous velocities of the hot spot along each spatial direction:

$$v_x(X, Y, Z, T) = \left. \frac{dx(t)}{dt} \right|_{t=0},$$

$$v_y(X, Y, Z, T) = \left. \frac{dy(t)}{dt} \right|_{t=0},$$

$$v_z(X, Y, Z, T) = \left. \frac{dz(t)}{dt} \right|_{t=0}. \quad (4)$$

These velocities correspond to the motion of the maximum of the hot spot and are functions of the macroscopic variables (X, Y, Z, T) because the field may be nonstationary relatively to the initial reference point. By injecting the parametric plot $\{x(t), y(t), z(t)\}$ into the FCF, we define a new function G , the maximum correlation function (MCF), which depends only on the time t and the macroscopic variables (X, Y, Z, T) :

$$G(X, Y, Z, T, t) = \Gamma(X, Y, Z, T, x(t), y(t), z(t), t). \quad (5)$$

This function G measures the correlation level between the initial hot spot maximum at (X, Y, Z, T) and the new hot spot maximum found in the space domain at a time t after the initial time T . We can then introduce the hot spot lifetime τ_f defined as the full width at half-maximum (FWHM) of G . τ_f can be considered the characteristic time of decrease of the MCF corresponding to the total extinction of the hot spot. People usually characterize the extinction time using the coherence time τ_c , which is the FWHM of the static correlation function F (SCF):

$$F(X, Y, Z, T, t) = \Gamma(X, Y, Z, T, 0, 0, 0, t). \quad (6)$$

However, the SCF evaluates the intensity at a particular point as a function of time and is therefore related to the optical contrast. The definition of the MCF implies that G always has a larger width than SCF. Then these temporal parameters verify the inequality

$$\tau_f \geq \tau_c. \quad (7)$$

If the hot spot turns off in place and does not move, the SCF is equal to the MCF and the hot spot lifetime is equal to the coherence time. However, τ_f can be much longer than τ_c if the hot spot moves without turning off. In the following sections we study different configurations and compare the MCF with the SCF. At this stage it is also useful to note that the coherence time is related to the spectrum bandwidth through the Wiener-Kyntchine theorem¹⁵:

$$I(\omega) = TF[\sqrt{F(X, Y, Z, T, t)}], \quad (8)$$

where TF is the Fourier transform related to t and $I(\omega)$ is the spectrum. We assume here that the spectrum has no spatial dependence; this has been verified in many cases. We can also find a relation between τ_c and the FWHM-spectrum bandwidth $\Delta\nu$ for different SCF shapes: $\tau_c = 0.62\Delta\nu^{-1}$ for a Gaussian shape and $\tau_c \cong 0.75\Delta\nu^{-1}$ for a sinusoidal phase modulation.

3. HOT SPOT MOTION FOR ONE-DIMENSIONAL SMOOTHING BY SPECTRAL DISPERSION

A. Principles

The 1D-SSD¹² is an efficient technique for creating time-varying speckle patterns, although it cannot provide a low contrast (the contrast typically stays higher than 20%).

The standard implementation is shown in Fig. 1. An incident monochromatic beam is spectrally broadened by a sinusoidal phase modulator with a frequency modulation ν_{mod} and a modulation depth m . The generated spectral bandwidth (FWHM) is then equal to $2m\nu_{\text{mod}}$. In the following, we call T_{mod} the modulation period, which is the inverse of ν_{mod} . By use of a grating, the spectrum is further dispersed onto a random-phase plate.¹⁶ The grating induces an angular dispersion along the transverse direction (x , in the following) with a resulting time delay T_d . The RPP consists of many elements that impose random phase shifts of 0 or π . The independent beamlets generated by the phase elements interfere in the focal plane and create a speckle pattern. Because of the grating,

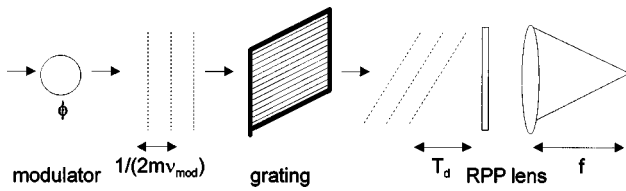


Fig. 1. Standard implementation of 1D-SSD.

each frequency focuses at a different point in the focus plane along the dispersion direction. As a result, the speckle pattern moves in time very quickly according to the spectral bandwidth. The asymptotic contrast for an optimized configuration, $T_d\nu_{\text{mod}} = 1$, is approximately $1/\sqrt{2m + 1}$. Introducing the number of color cycles N_c defined as the ratio between T_d and T_{mod} , the asymptotic contrast is obtained as soon as N_c is equal to 1. This value is therefore called the critical dispersion.

B. Hot Spot Motion with a Sinusoidal Phase Modulation

In this subsection we consider a pure sinusoidal phase modulation $\phi(t) = m \sin(2\pi\nu_{\text{mod}}t)$. In Appendix A we give a theoretical result for the FCF in the 1D-SSD configuration [Eq. (A3)]. In Fig. 2 we present the FCF at time $t = 1.4$ ps for a case corresponding to the LMJ configuration, with a square near-field beam and a focus length f_0 equal to 8 m, the width D of the beam before focusing is 0.91 m. The modulation depth m is 10 and the frequency modulation ν_{mod} is 10 GHz. We assume also that the time delay T_d is the inverse of ν_{mod} . These values correspond to a spectral bandwidth of 200 GHz centered at $\lambda_0 = 351$ nm. The initial reference point is the

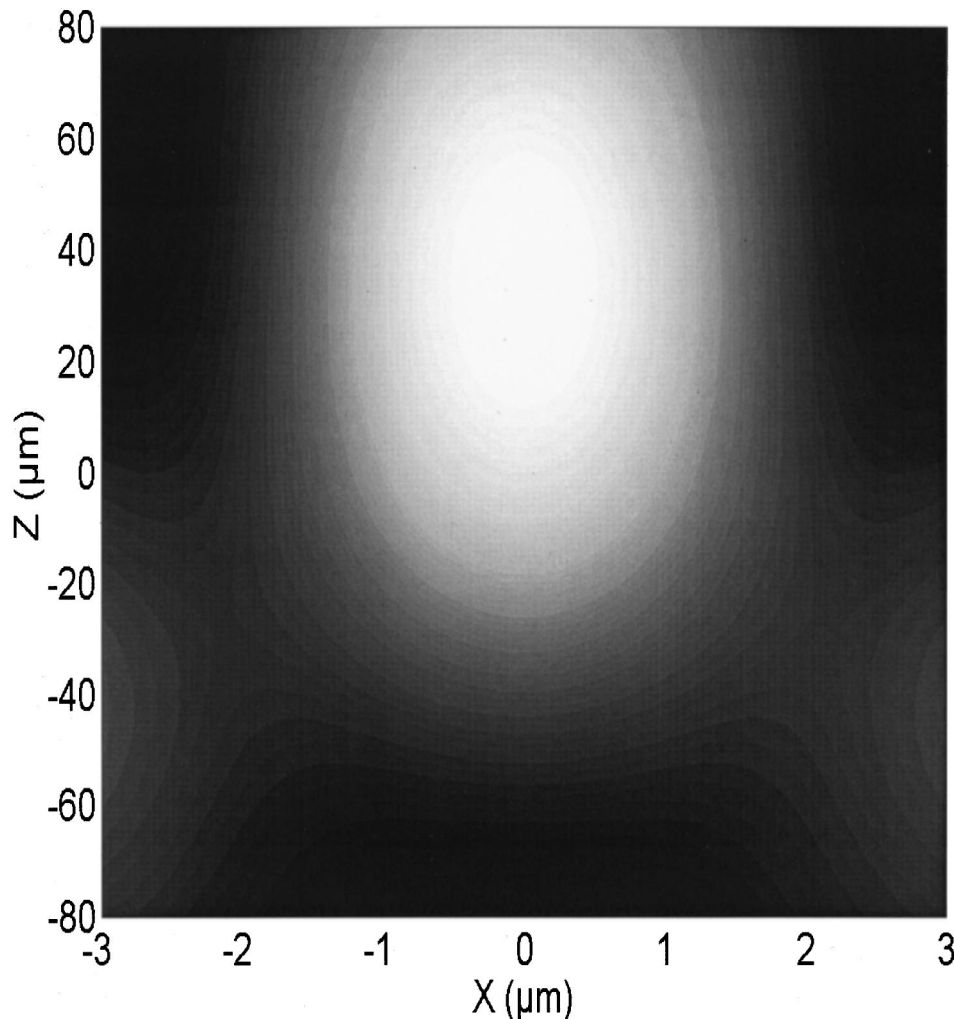


Fig. 2. FCF for 1D-SSD with a sinusoidal phase modulation at $t = 1.4$ ps. In this case $m = 10$, $\nu_{\text{mod}} = 10$ GHz, $\lambda_0 = 351$ nm, $T_d = 100$ ps, $D = 0.91$ m, $f_0 = 8$ m. The initial time T is $T_{\text{mod}}/2$, and the initial point reference is the focus: $(X, Y, Z) = (0, 0, 0)$. For $t = 0$, the hot spot is centered at $z = x = 0$.

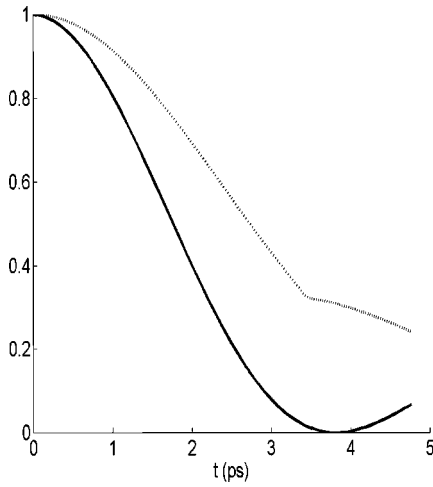


Fig. 3. Comparison of the MCF and the SCF. Dotted curve, MCF; solid curve, SCF. The parameters are the same as in Fig. 2.

center of the focal volume, and the initial time T is 50 ps, which is the half-period of one modulation.

In Fig. 2 we show the motion of the maximum of the FCF along the longitudinal direction: The hot spot moves and does not turn off in place. The longitudinal velocity is ~ 0.088 of the light velocity c ; there is no motion in the transverse direction. In Fig. 3 we have plotted the MCF and the SCF. We observe a difference between these functions, the width of the MCF always being larger than that of the SCF. The coherence time τ_c is 3.5 ps, and the hot spot lifetime τ_f is equal to 5.5 ps, which is longer than τ_c by a factor of 1.55. At roughly 3 ps, the MCF presents a break corresponding to the correlation with a newly appearing hot spot. Nevertheless this breakpoint corresponds to a low value of the correlation where the validity of Adler's theorem (Section 2) is not very accurate.

C. Calculations of Velocities and Hot Spot Lifetime

In Subsection 3.B we showed a hot spot moving in the forward direction without transverse components. In fact, the motion for 1D-SSD depends strongly on the initial time T . In particular, we have a backward motion if T is null and an almost transverse one when T is equal to $0.25 T_{\text{mod}}$ or $0.75 T_{\text{mod}}$. Finally, we have a combination of transverse and longitudinal motions for other values of T . In Appendix B we obtain theoretical results for the instantaneous velocities and hot spot lifetime by developing Eq. (2), assuming the initial point as the focus point: $(X, Y, Z) = (0, 0, 0)$. The averaged velocity v_x along the dispersion direction is

$$v_x(0, 0, 0, T)$$

$$= c \frac{3R_{\text{lat}}C_4 \sin\left(2\pi \frac{T}{T_{\text{mod}}}\right) \left[\frac{1}{45} + \frac{R_{\text{long}}}{\pi} \cos\left(2\pi \frac{T}{T_{\text{mod}}}\right) C_1 \right]}{\frac{1}{45} + 2 \frac{R_{\text{long}}}{\pi} \cos\left(2\pi \frac{T}{T_{\text{mod}}}\right) C_1 + \frac{R_{\text{long}}^2}{\pi^2} C\left(\frac{T}{T_{\text{mod}}}\right)}, \quad (9)$$

where

$$R_{\text{lat}} = \frac{\rho_0}{z_c}, \quad R_{\text{long}} = \frac{z_0}{z_c}, \quad \rho_0 = \frac{2\pi f}{k_0 D},$$

$$z_0 = \frac{k_0 \rho_0^2}{2}; \quad z_c = \frac{c T_{\text{mod}}}{2m}. \quad (10)$$

The coefficients C_j and C depend on N_c , the number of color cycles being equal to the ratio T_d/T_{mod} . We get

$$C(u) = C_2 - 6C_4^2 + \cos(2\pi u)^2(C_3 + 6C_4^2).$$

The expressions of the functions C_j are

$$C_1 = \frac{\cos(\pi N_c)}{(\pi N_c)^2} - \frac{\sin(\pi N_c)}{(\pi N_c)^3} + \frac{1}{3} \frac{\sin(\pi N_c)}{\pi N_c};$$

$$C_2 = 1 - \frac{\sin(2\pi N_c)}{2\pi N_c};$$

$$C_3 = 2 \frac{\sin(2\pi N_c)}{2\pi N_c} - 2 \frac{\sin(\pi N_c)^2}{(\pi N_c)^2};$$

$$C_4 = \frac{\sin(\pi N_c)}{(\pi N_c)^2} - \frac{\cos(\pi N_c)}{(\pi N_c)}.$$

The velocity along the transverse direction y is null. We obtain the expression of the longitudinal velocity v_z :

$$v_z(0, 0, 0, T)$$

$$= c \frac{\frac{R_{\text{long}}}{\pi} \cos\left(2\pi \frac{T}{T_{\text{mod}}}\right) C_1 + \frac{R_{\text{long}}^2}{\pi^2} C\left(\frac{T}{T_{\text{mod}}}\right)}{\frac{1}{45} + 2 \frac{R_{\text{long}}}{\pi} \cos\left(2\pi \frac{T}{T_{\text{mod}}}\right) C_1 + \frac{R_{\text{long}}^2}{\pi^2} C\left(\frac{T}{T_{\text{mod}}}\right)}. \quad (11)$$

Given that both velocities depend on the initial time T , the instantaneous velocities vary during the modulation period. Furthermore, they depend strongly on the number of color cycles because of the functions C_j . For a large value of N_c (large meaning greater than 2), the functions C_1 , C_3 , and C_4 are close to 0, whereas the function C_2 has an almost constant value of 1. The transverse velocity becomes null and the longitudinal one is given by the asymptotic expression

$$v_z(0, 0, 0, T) = c \frac{R_{\text{long}}^2}{\pi^2 + R_{\text{long}}^2} = c \frac{1}{1 + \frac{\pi^2}{45} \left(\frac{z_c}{z_0}\right)^2}. \quad (12)$$

Actually, all characteristic quantities become independent of T when $N_c \gg 1$, because the field in the focal spot results from the superposition of many different beamlets that correspond to different times, so that this time integration averages the local dependence to 0. Using Eqs.

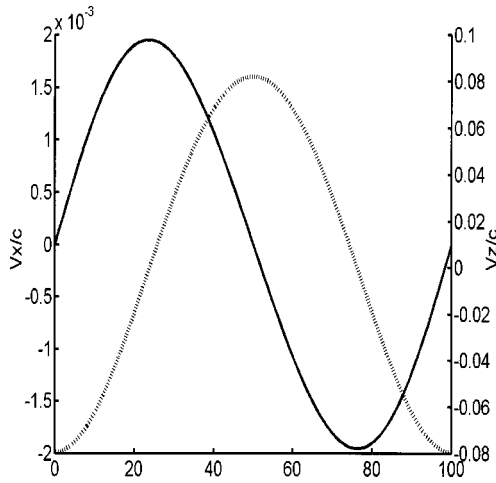


Fig. 4. Transverse velocity v_x (solid curve) and longitudinal velocity v_z (dotted curve) as a function of the initial time T with $N_c = 1$.

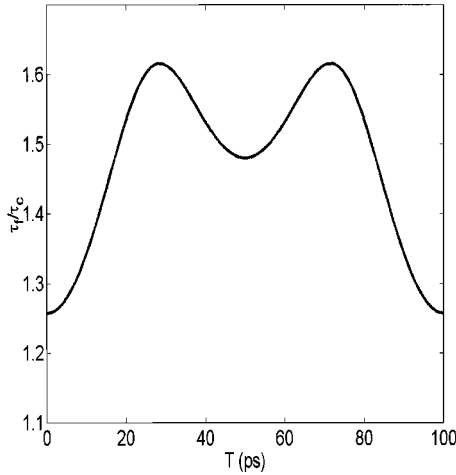


Fig. 5. Ratio between the hot spot lifetime and the coherence time as a function of the initial time T .

(9) and (11), in Fig. 4 we have plotted the transverse and the longitudinal velocities as a function of the initial time T . The laser parameters are the same as in the case shown in Subsection 3.B. In particular, at $T = T_{\text{mod}}/2$, we find that $v_z = 0.08c$ and $v_x = 0$, which is in good agreement with the values found in Subsection 3.B. In these conditions the motion is essentially in the forward or the backward longitudinal direction, because v_z is much larger than v_x .

By expanding the expressions of $G(t)$ and $F(t)$ with respect to t , we can estimate the ratio τ_f/τ_c , where τ_f is the hot spot lifetime [i.e., the width of $G(t)$] and τ_c is the coherence time (i.e., the width of $F(t)$):

$$\tau_f/\tau_c = \sqrt{D_0(T)/D(T)}, \quad (13)$$

where the expressions of $D(T)$ and $D_0(T)$ are given in Appendix B. Figure 5 presents the ratio plotted as a function of T for the case in Fig. 4.

The ratio depends on time and is maximal for $T = 0.25T_{\text{mod}}$, a case that corresponds to a purely transverse motion. For any initial time T , the hot spot lifetime is longer than the coherence time, with a maximum ratio of 1.62. At half-period, the asymptotic relation

gives a ratio of 1.48, which is close to the 1.55 value found in Subsection 3.B. So the asymptotic relations are in good agreement with the calculated ones in term of instantaneous velocities and ratio between the hot spot lifetime and the coherence time. We have assumed here only that the hot spot was initially at the center of the focal volume and that the phase modulation was a pure sinusoidal modulation. In the following subsection we study the effect of an incoherent spectrum.

D. Effect of an Incoherent Spectrum

In Subsections 3.B and 3.C we have studied the case of a sinusoidal phase modulation, which is basic laser technology. Here we assume that the different frequencies in the spectrum are incoherent while the spectral intensity is the same. This field is written as

$$\begin{aligned} \tilde{E}(\nu) = \int E(t) \exp(2i\pi\nu t) dt = \sum_{n=-\infty}^{+\infty} \exp(i\varphi_n) J_n(m) \\ \times \delta(\nu - n\nu_{\text{mod}}), \end{aligned} \quad (14)$$

where φ_j are random phases and J_n are Bessel functions. The spectrum is incoherent, but the spectral intensity is the same as with sinusoidal modulations. There is then almost no motion of the hot spot, and the hot spot lifetime is reduced to a value very close to the coherence time. The effect of the incoherent spectrum is to inhibit any temporal correlation that is due to a deterministic relation such as a sinusoidal phase modulation. This means that to limit hot spot motions it is relevant to use a random-phase modulation and avoid a pure sinusoidal one.

4. HOT SPOT MOTION FOR SMOOTHING BY LONGITUDINAL SPECTRAL DISPERSION

A. Principles

In LMJ design, the focusing is performed by a grating that directly disperses the third harmonic,¹⁷ and the beam shape is square. This configuration offers many advantages, such as color separation and an improvement of the frequency-conversion efficiency. Furthermore, the grating provides a focal length that depends on the frequency ω ¹⁸:

$$f(\omega) = \frac{\omega + \omega_0}{\omega_0} f_0, \quad (15)$$

where f_0 is the focal length for the central frequency ω_0 . The grating is tailored so that more than 90% of the energy is focused in the central spot.¹⁷ The grating is then equivalent to a chromatic lens, and its transmission function^{19,20} T is in the paraxial approximation:

$$\begin{aligned} T(x, y, z, \omega) = \exp\left[-i \frac{k_0(x^2 + y^2)}{2f(\omega)}\right] \\ \approx \exp\left[-i \frac{k_0(x^2 + y^2)}{2f_0} \left(1 - \frac{\omega}{\omega_0}\right)\right]. \end{aligned} \quad (16)$$

We can introduce the maximal time delay T_d between the edge and the center of the beam given by the relation

$$T_d = \frac{k_0}{2f_0\omega_0} [(D/2)^2 + (D/2)^2] = \frac{D^2}{4f_0c}. \quad (17)$$

Each frequency in the spectrum focuses at a particular point along the z axis (Fig. 6). Two different frequencies create independent speckle patterns if the difference between their focal lengths is larger than the longitudinal speckle dimension. In fact, smoothing by longitudinal spectral dispersion (SLSD) belongs to the 1D-SSD category but with a spectral dispersion along the longitudinal instead of the transverse direction.

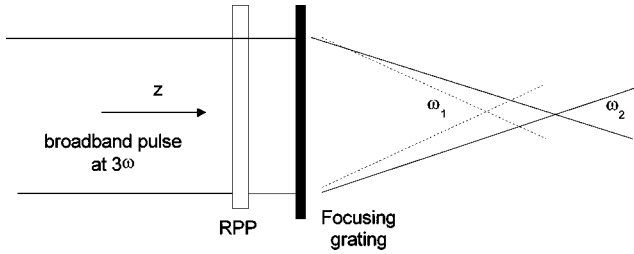


Fig. 6. Standard implementation of a focusing grating.

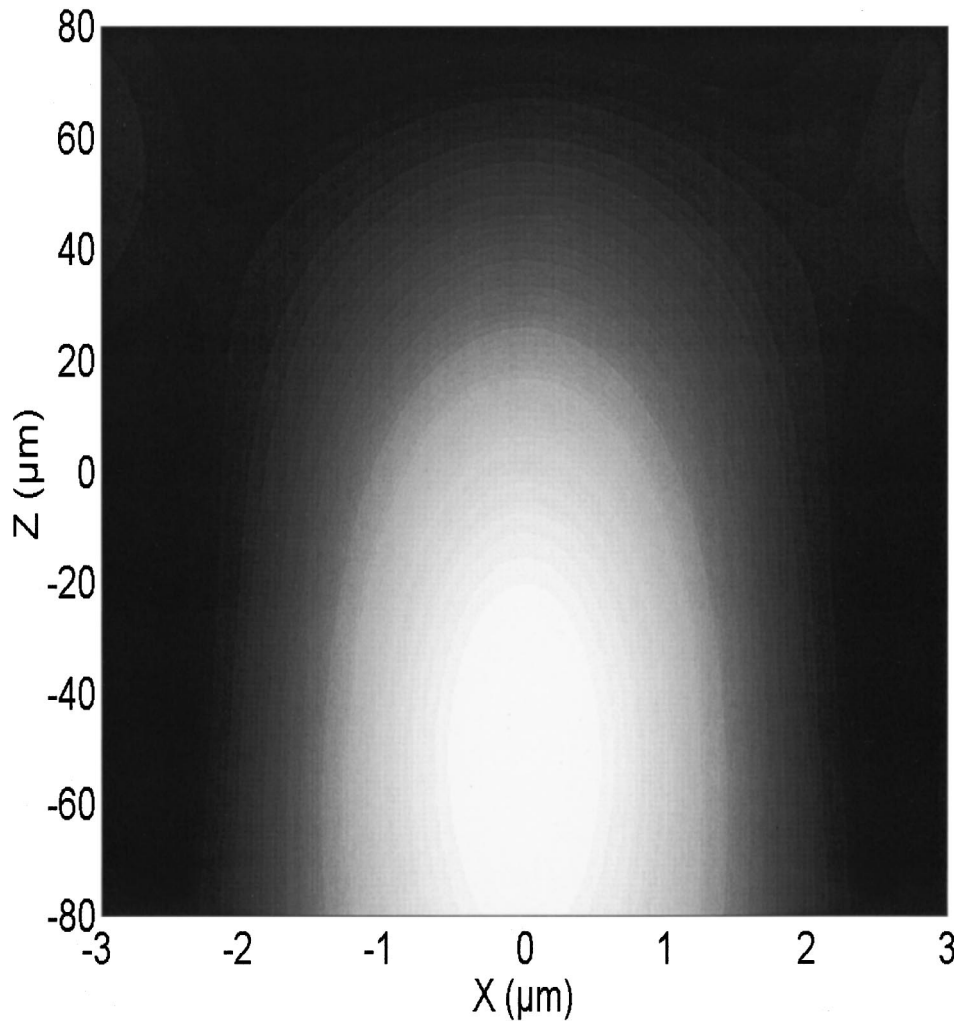


Fig. 7. FCF for SLSD with a sinusoidal phase modulation at $t = 1.4$ ps. In this case $m = 10$, $\nu_{\text{mod}} = 10$ GHz, $\lambda_0 = 351$ nm, $T_d = 86$ ps, $D = 0.91$ m, $f_0 = 8$ m. The initial time T is null and the initial point reference is the focus: $(X, Y, Z) = (0, 0, 0)$. For $t = 0$, the hot spot is centered at $z = x = 0$.

B. Hot Spot Motion with a Sinusoidal Phase Modulation

We studied the case presented in Subsection 3.B, that with a pure sinusoidal phase modulation. We assume that the time delay is defined by Eq. (17), $T_d = 86$ ps. For this technique there is only a longitudinal motion in the forward or backward direction owing to the absence of a transverse dispersion. In the case of Fig. 7 the motion is backward, with an instantaneous velocity equal to $v_z = -0.112c$. In Fig. 8 we have plotted the MCF and the SCF for $T = 0$. The width of the MCF is larger than that of the SCF, the ratio τ_f/τ_c being 5.32. Actually, this motion depends on the sinusoidal phase modulation, which still exists locally in the focal volume. The use of an incoherent spectrum such as the one in Subsection 3.D limits the motion and decreases the hot spot lifetime. Indeed, the results for 1D-SSD with an incoherent spectrum are the same for SLSD, in which case the difference between τ_f and τ_c is also drastically reduced.

C. Calculations of Velocities and Hot Spot Lifetime

We obtained asymptotic results by developing the same calculations presented in Appendix B and in Subsection

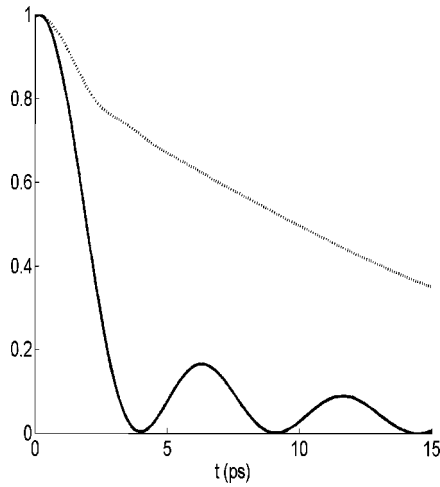


Fig. 8. Comparison of the MCF and the SCF. Dotted curve, MCF; solid curve, SCF. The parameters are the same as in Fig. 7.

3.C for 1D-SSD. In particular, we obtained a simplified expression of Eq. (A3):

$$\begin{aligned} \gamma(\boldsymbol{\rho}, z, t, T) &= \Gamma\left(\frac{x}{2}, \frac{y}{2}, \frac{z}{2}, T + \frac{t}{2}, -\frac{x}{2}, -\frac{y}{2}, -\frac{z}{2}, T - \frac{t}{2}\right) \\ &\propto \left| \int \int_{D(0,1)} \exp[i(A + D)] d^2u \right|^2, \end{aligned} \quad (18)$$

where

$$\begin{aligned} A &= \pi \frac{\mathbf{u} \cdot \boldsymbol{\rho}}{\rho_0} - \pi^2 \frac{z}{4z_0} \mathbf{u} \cdot \mathbf{u}, \\ D &= 2m \sin\left(\pi \frac{t - z/c}{T_{\text{mod}}}\right) \cos\left(2\pi \frac{T}{T_{\text{mod}}} - \pi N_c \mathbf{u} \cdot \mathbf{u}\right), \end{aligned}$$

with $N_c = T_d/T_{\text{mod}}$, T_d given by Eq. (17).

We find that the transverse velocities v_x and v_y are always null, and the expression of the longitudinal velocity v_z is

$$\begin{aligned} v_z(0, 0, 0, T) &= c \frac{\frac{R_{\text{long}}}{2\pi} (D_1 + D_2) + \frac{R_{\text{long}}^2}{4\pi^2} (D_3 + D_4 + D_5)}{\frac{1}{45} + \frac{R_{\text{long}}}{\pi} (D_1 + D_2) + \frac{R_{\text{long}}^2}{4\pi^2} (D_3 + D_4 + D_5)}, \end{aligned} \quad (19)$$

where the D_j depend on N_c and T .

$$\begin{aligned} D_1 &= \cos\left(\frac{2\pi T}{T_{\text{mod}}}\right) \left[C_s \frac{\sin(\pi N_c)}{\pi N_c} \right. \\ &\quad \left. + S_s \frac{\cos(\pi N_c)}{\pi N_c} - \frac{2C_s S_s}{\pi N_c} - \frac{2}{3} (C_s^2 - S_s^2) \right], \end{aligned}$$

$$\begin{aligned} D_2 &= \sin\left(\frac{2\pi T}{T_{\text{mod}}}\right) \left[S_s \frac{\sin(\pi N_c)}{\pi N_c} - C_s \frac{\cos(\pi N_c)}{\pi N_c} \right. \\ &\quad \left. + \frac{C_s^2 - S_s^2}{\pi N_c} - \frac{4}{3} C_s S_s \right], \end{aligned}$$

$$D_3 = \cos\left(\frac{4\pi T}{T_{\text{mod}}}\right) [C_s^2 - S_s^2 - 4(C_s^2 + S_s^2)^2],$$

$$D_4 = 2 \sin\left(\frac{4\pi T}{T_{\text{mod}}}\right) C_s S_s [1 - 8(C_s^2 - S_s^2)],$$

$$D_5 = 4[1 - (C_s^2 + S_s^2)^2],$$

where

$$C_s = \frac{1}{\sqrt{2N_c}} \int_0^{\sqrt{2N_c}} \cos\left(\frac{\pi}{2} t^2\right) dt,$$

$$S_s = \frac{1}{\sqrt{2N_c}} \int_0^{\sqrt{2N_c}} \sin\left(\frac{\pi}{2} t^2\right) dt.$$

For a large value of N_c , the functions C_s and S_s are null and the longitudinal velocity v_z becomes

$$v_z(0, 0, 0, T) = c \frac{R_{\text{long}}^2}{\frac{\pi^2}{45} + R_{\text{long}}^2} = c \frac{1}{1 + \frac{\pi^2}{45} \left(\frac{z_c}{z_0}\right)^2}, \quad (20)$$

which is the same expression as Eq. (12) for 1D-SSD.

In Fig. 9 using Eq. (19), we have plotted the longitudinal velocity as a function of initial time T , with N_c equal to 1. For $T = 0$ we find a velocity equal to $-0.112c$, which corresponds to the value found in subsection 4.2. v_z oscillates between $0.105c$ and $-0.125c$ with the period of the phase modulator. With this technique we can not apply the same approach as with 1D-SSD for evaluating the lifetime. Indeed, the shape of the MCF can not be fitted by a Gaussian function (Fig. 8), because the MCF presents an anomalous break (at $t = 2$ ps in Fig. 8), which strongly enhances its FWHM. We then have to compute the MCF numerically by using the complete formula of the FCF defined in Eq. (18). In Fig. 10 we have plotted

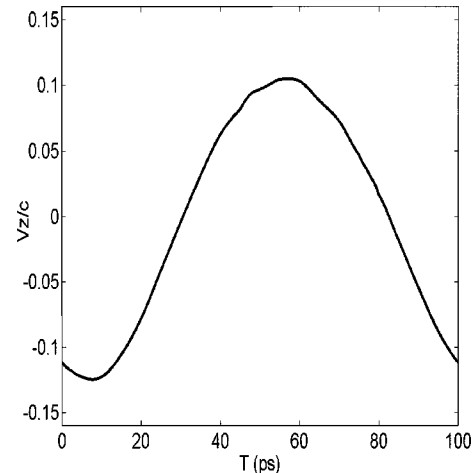


Fig. 9. Longitudinal velocity v_z as a function of the initial time T with $N_c = 1$, using Eq. (19). The parameters are as in Fig. 7.

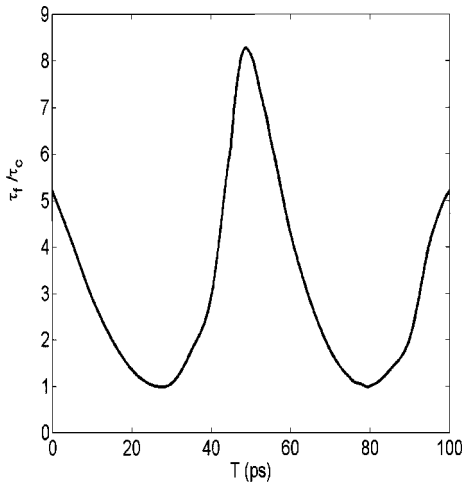


Fig. 10. Ratio between τ_f and τ_c as a function of the initial time T with $N_c = 1$ obtained by computing the FCF [Eq. (18)]. The parameters are the same as in Fig. 7.

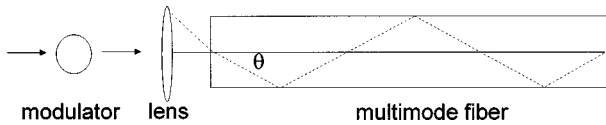


Fig. 11. Standard implementation of SOF.

the ratio between τ_f and τ_c for the case presented in Fig. 7. The hot spot lifetime is always longer than the coherence time, with a maximum value of eight times the coherence time. In this case the hot spot does not turn off in place but propagates.

5. HOT SPOT MOTION FOR SMOOTHING BY OPTICAL FIBER

A. Principles

Smoothing by optical fiber^{4,5} (SOF) is used to obtain a low contrast (<10%) when one-dimensional techniques such as 1D-SSD or SLSD are not efficient. In this method a time-incoherent pulse is injected into a long multimode optical fiber and excites many optical modes that propagate at different angles (Fig. 11). At the output of the fiber the modes are independent because of the random phases encountered in the fiber, and their overlap produces a speckle pattern. Furthermore, the spatial modes have a specific propagation time in the core of the fiber that is due to the different angles of propagation, the maximum time delay being $T_d = L\theta^2/2nc$, where L is the length of the fiber, θ is the maximal incident angle, and n is the fiber index.

Generally, the time delay is chosen of the same order as the pulse duration, which is typically 1 ns or above. For asymptotic contrast and the speckle motion, the shape and the width of the spectrum are then the only relevant parameters, and a sinusoidal phase modulation provides the same kind of behavior as an incoherent spectrum with the same spectral bandwidth.

B. Statistical Results

The hot spot motion for SOF is very close to the 1D-SSD or the SLSD case when an incoherent spectrum is used.

By the same method as in Section 3, we can show that the motion occurs only along the z axis with an instantaneous velocity given by

$$v_z = \frac{c}{1 + \frac{\pi^2}{96} \left(\frac{z_c}{z_0}\right)^2}. \quad (21)$$

z_c and z_0 are defined by Eq. (10). Equation (21) differs from Eqs. (12) and (20) by an adimensional constant 96/45 that originates from geometrical considerations. The field at the output of the fiber has a circular shape, whereas the near-field beam is assumed to be square in the 1D-SSD configuration. z_c corresponds to the laser coherence length and z_0 to the Rayleigh parameter.

If z_c is much larger than z_0 , the hot spot tube is filled by a single pulse. The hot spot turns off because of smoothing, the lifetime being close to the coherence time. The velocity given by Eq. (21) becomes small compared with the light velocity.

However if z_c is now lower than z_0 , a temporal coherent pulse illuminates only a small section of the hot spot tube. This section of longitudinal width z_0 propagates with a velocity close to the light velocity [Eq. (21)]. The propagation distance is then the Rayleigh dimension, the hot spot lifetime being the propagation time of the section up to the “end” of the speckle. In this condition, we find that the hot spot lifetime is equal to $\tau_f = z_0/c$. In fact, the hot spot motion for SOF is essentially related to the interplay between the diffraction and the longitudinal coherence length of the laser, and the exact expression of τ_f/τ_c computed by the same method as in Subsection 3.C is

$$\frac{\tau_f}{\tau_c} = \left[1 + \frac{96}{\pi^2} \left(\frac{z_0}{z_c}\right)^2 \right]^{1/2}. \quad (22)$$

The same arguments can be applied to the 1D-SSD configuration if the time delay is longer than the modulation period ($N_c \gg 1$).

6. CONCLUSIONS

We have developed a statistical approach for studying hot spot motion with use of all the smoothing techniques. Section 2 introduces new definitions such as the four-dimensional correlation function (FCF) and the maximum correlation function (MCF). The FCF allows us to describe temporally and spatially the shape of a local maximum of intensity (i.e., a hot spot). In particular, we can evaluate the instantaneous velocities in the transverse and longitudinal directions. Furthermore, the MCF gives at each time the correlation of the hot spot with the initial hot spot. The decrease of the MCF is given by the hot spot lifetime, which measures the correlation in the moving reference frame of the maximum of intensity. It is important to compare this parameter with the coherence time, which is the inverse of the spectrum bandwidth. Indeed, we have shown in Sections 3 and 4 that τ_f can be longer than τ_c for smoothing techniques such as 1D-SSD and SLSD when sinusoidal phase modulation is used. This means that the hot spot moves in time without turning off immediately. In some conditions this be-

havior may enhance the parametric instabilities whose growth is much more important at the maximum of intensity. Thus a knowledge of the velocities and the hot spot lifetime is important for evaluating the influence of laser intensity on the plasma. Furthermore, we have shown that the SOF technique presents no increase in correlation that is due to a sinusoidal phase modulation. Only the interplay of diffraction and laser coherence length is relevant in this case.

APPENDIX A

In this appendix we present the computation of the FCF defined by Eq. (A1) for 1D-SSD and SLSD:

$$\Gamma(x_1, y_1, z_1, t_1, x_2, y_2, z_2, t_2) = \frac{|\langle E(x_1, y_1, z_1, t_1)E^*(x_2, y_2, z_2, t_2) \rangle|^2}{\langle I(x_1, y_1, z_1, t_1) \rangle \langle I(x_2, y_2, z_2, t_2) \rangle}. \quad (\text{A1})$$

The effect of the first grating used for 1D-SSD is to induce a time delay T_d along the x axis so that the field after the grating becomes $E_0(x, y, z, t + T_d x/D)$, where E_0 is the initial field and D is the width of the beam. We assume that E_0 depends only on the time and is a plane wave in the spatial domain. The random phase plate placed just before the focusing component has a transmission function of the form

$$M(x, y) = \sum_{n,m=1}^N \exp(i\varphi_{n,m})S(x - na)S(y - na), \quad (\text{A2})$$

where $\varphi_{n,m}$ are independent random phases and S is the geometrical shape of one element with a width equal to a . N is the number of elements along one direction. To simplify the computations, we assume that S is Gaussian in shape. This parameter is relevant only for the envelope of the focused beam and not for the hot spot shape. Finally, we introduce the focusing grating as a chromatic lens with a transmission function $T(x, y, \omega) = \exp[-i(x^2 + y^2)k_0/2f(\omega)]$, where $f(\omega)$ is given by Eq. (15). The propagation is taken care of with a Fourier transform formalism.^{19,20} If we assume that $N \rightarrow +\infty$, we can replace the discrete sums by continuous integrals, which yields the FCF expression,

$$\Gamma(x_1, y_1, z_1, t_1, x_2, y_2, z_2, t_2) \propto \left| \iint \tilde{E}_0(\omega_1)\tilde{E}_0^*(\omega_2) \times \exp\left[i\omega_2\left(t_2 - \frac{z_2}{c}\right) - i\omega_1\left(t_1 - \frac{z_1}{c}\right)\right] \times p_x(1; 2)p_y(1; 2)d\omega_1d\omega_2 \right|^2, \quad (\text{A3})$$

where $\tilde{E}_0(\omega) = \int E_0(t)\exp(i\omega t)dt$ and \propto means "is proportional to."

$$p_u(1; 2) = p(u_1, z_1, \omega_1, u_2, z_2, \omega_2) = \frac{1}{D} \exp\left(i \frac{\delta g^2 f_0}{2k_0 |\delta h|}\right) \times \int_{-D/2 + \delta g f_0 / k_0 \delta h}^{D/2 + \delta g f_0 / k_0 \delta h} \exp\left[-i \frac{k_0 \delta h}{2f_0} s^2\right] ds, \quad (\text{A4})$$

where u means x or y , $\delta g = (\omega_1 - \omega_2)T_d^u/D - (u_1 - u_2)k_0/f_0$, and $\delta h = z_1 - z_2/f_0 - (\omega_1 - \omega_2)/\omega_0$. T_d^u is the time delay along the transverse direction u (x or y), and ω_0 is the central frequency.

APPENDIX B

Here we compute the asymptotic developments of Eq. (A3) for the case of 1D-SSD when a pure sinusoidal phase modulation is used. Note that the lens in this configuration is standard so that the focal length does not depend on ω . Furthermore we assume that the initial hot spot is centered in the focal volume: $(X, Y, Z) = (0, 0, 0)$. In these conditions, we have a simplified expression of Eq. (A3):

$$\gamma(\boldsymbol{\rho}, z, t, T) = \Gamma\left(\frac{x}{2}, \frac{y}{2}, \frac{z}{2}, T + \frac{t}{2}, -\frac{x}{2}, -\frac{y}{2}, -\frac{z}{2}, T - \frac{t}{2}\right) \propto \left| \iint_{D(0,1)} \exp[i(A + B)]d^2u \right|^2, \quad (\text{B1})$$

with $\boldsymbol{\rho} = (x, y)$, $\mathbf{u} = (u_1, u_2)$, $\rho_0 = 2\pi f/k_0 D$, $z_0 = k_0 \rho_0^2/2$.

$$A = A(\mathbf{u}) = \pi \frac{\mathbf{u} \cdot \boldsymbol{\rho}}{\rho_0} - \pi^2 \frac{z}{4z_0} \mathbf{u} \cdot \mathbf{u},$$

$$B = B(\mathbf{u}) = 2m \sin\left(\pi \frac{t - z/c}{T_{\text{mod}}}\right) \times \cos\left(2\pi \frac{T}{T_{\text{mod}}} + \pi N_c u_1\right).$$

$D(0,1)$ represents the integration domain and is the unity square, which is the shape of the near-field beam. The derivative functions of γ are proportional to

$$\frac{\partial \gamma}{\partial z} \propto \iint_{D(0,1)} \cos(A + B)d^2u \times \iint_{D(0,1)} \left[\frac{\partial(A + B)}{\partial z} \right] \times \sin(A + B)d^2u - \iint_{D(0,1)} \sin(A + B)d^2u \times \iint_{D(0,1)} \left[\frac{\partial(A + B)}{\partial z} \right] \times \cos(A + B)d^2u,$$

$$\begin{aligned} \frac{\partial \gamma}{\partial \rho_j} \propto & \int \int_{D(0,1)} \cos(A+B) d^2u \times \int \int_{D(0,1)} u_j \\ & \times \sin(A+B) d^2u - \int \int_{D(0,1)} \\ & \times \sin(A+B) d^2u \times \int \int_{D(0,1)} u_j \\ & \times \cos(A+B) d^2u. \end{aligned}$$

The maximum of the hot spot is the point $(\boldsymbol{\rho}, z)$, where the three derivatives functions of γ with respect to ρ_1 , ρ_2 , and z vanish. We assume from now on that $t \ll T_{\text{mod}}$ in order to evaluate the instantaneous velocities, and we develop cosines and sines at first order near $(\boldsymbol{\rho}, z, t) = (\mathbf{0}, 0, 0)$. After some developments we find the position of the intensity maximum:

$$x(t) = v_x t + O(t^2); \quad y(t) = 0, \quad z(t) = v_z t + O(t^2),$$

where v_x and v_z are given, respectively, by Eq. (9) and Eq. (11). By injecting the previous results into Eq. (B1), we find the maximum correlation function G :

$$G(t, T) = 1 - 2\pi^2 m^2 \frac{t^2}{T_{\text{mod}}^2} D(T) + O\left(m^4 \frac{t^4}{T_{\text{mod}}^4}\right), \quad (\text{B2})$$

with

$$D(T) = \frac{\frac{1}{45} C \left(\frac{T}{T_{\text{mod}}}\right) - \cos\left(2\pi \frac{T}{T_{\text{mod}}}\right)^2 C_1}{\frac{1}{45} + 2 \frac{R_{\text{long}}}{\pi} \cos\left(2\pi \frac{T}{T_{\text{mod}}}\right) C_1 + \frac{R_{\text{long}}^2}{\pi^2} C \left(\frac{T}{T_{\text{mod}}}\right)}.$$

Finally, we compute the static correlation function F :

$$F(t, T) = 1 - 2\pi^2 m^2 \frac{t^2}{T_{\text{mod}}^2} D_0(T) + O\left(m^4 \frac{t^4}{T_{\text{mod}}^4}\right), \quad (\text{B3})$$

with $D_0(T) = C_2 + \cos[2\pi(T/T_{\text{mod}})]^2 C_3$.

ACKNOWLEDGMENTS

We thank C. Gouedard and C. Sauteret for useful and stimulating discussions. This work was performed under the auspices of the Laser MegaJoule Program of Commissariat à l'Énergie Atomique/Direction des Applications Militaires (CEA/DAM).

Send correspondence to L. Videau by phone, 33-5-56-68-4352; fax, 33-5-57-71-5463; or e-mail, videau@limeil.cea.fr.

*Present address, Commissariat à l'Énergie Atomique, Centre d'Étude Scientifique et Technique d'Aquitaine, BP No. 2, 33114 Le Barp, France.

REFERENCES

1. R. H. Lehmberg and S. P. Obenschain, "Use of induced spatial incoherency for uniform illumination," *Opt. Commun.* **46**, 27–31 (1983).
2. R. H. Lehmberg and J. Goldhar, "Use of incoherence to produce smooth and controllable irradiation profiles with KrF fusion lasers," *Fusion Technol.* **11**, 532–541 (1987).
3. A. V. Deniz, T. Lehecka, R. H. Lehmberg, and S. P. Obenschain, "Comparison between measured and calculated nonuniformities of Nike laser beams smoothed by induced spatial incoherence," *Opt. Commun.* **147**, 402–410 (1998).
4. D. Veron, G. Thiell, and C. Gouedard, "Optical smoothing of the high power Phebus Nd-glass laser using the multimode optical fiber technique," *Opt. Commun.* **97**, 259–271 (1993).
5. J. Garnier, L. Videau, C. Gouedard, and A. Migus, "Statistical analysis for beam smoothing and some applications," *J. Opt. Soc. Am. A* **14**, 1928–1937 (1997).
6. J. E. Rothenberg, "Two-dimensional smoothing by spectral dispersion for direct drive inertial confinement fusion," in *Solid State Lasers for Applications to ICF*, M. André and H. Powell, eds., Proc. SPIE **2633**, 634–644 (1995).
7. M. André, "Mégajoule solid state laser for ICF applications," in *Technical Committee Meeting on Drivers and Ignition Facilities for Inertial Fusion*, J. Coutant, ed., Proceedings of the International Atomic Energy Agency (CEA/DAM Publications, Limeil-Valenton, France, 1995), pp. 77–78.
8. J. E. Rothenberg, "A comparison of beam smoothing for direct drive inertial confinement fusion," *J. Opt. Soc. Am. B* **14**, 1664–1671 (1997).
9. S. N. Dixit, M. D. Feit, M. D. Perry, and H. T. Powell, "Designing fully continuous phase screens for tailoring focal-plane irradiance profiles," *Opt. Lett.* **21**, 1715–1717 (1996).
10. A. C. Newell and J. V. Moloney, *Nonlinear Optics* (Addison-Wesley, Redwood City, Calif., 1992).
11. E. Lefebvre, R. L. Berger, A. B. Langdon, B. J. McGowan, J. E. Rothenberg, and E. A. Williams, "Reduction of laser self-focusing in plasma by polarization smoothing," *Phys. Plasmas* **5**, 2701–2705 (1998).
12. S. Skupsky, R. W. Short, T. Kessler, R. S. Craxton, S. Letzring, and J. M. Soures, "Improved laser-beam uniformity using the angular dispersion of frequency-modulated light," *J. Appl. Phys.* **66**, 3456–3462 (1989).
13. J. Adler, *Geometry of Random Fields* (Wiley, New York, 1981).
14. H. A. Rose and D. F. DuBois, "Statistical properties of laser hot spots produced by a random phase plate," *Phys. Fluids B* **5**, 590–596 (1993).
15. D. Middleton, *Introduction to Statistical Communication Theory* (McGraw-Hill, New York, 1960).
16. Y. Kato and K. Mima, "Random phase shifting of laser beam for absorption profile smoothing and instability suppression in laser produced plasmas," *J. Appl. Phys.* **29**, 186–178 (1982).
17. A. C. L. Boscheron, E. Journot, A. Dulac, and A. Adolf, "Grating-based broadband third-harmonic generation and focusing system for the Laser Mégajoule," in *Conference on Lasers and Electro-Optics*, Vol. 6 of OSA Technical Digest Series (Optical Society of America, Washington, D.C., 1998), pp. 342–343.
18. Z. Bor, "Distortion of femtosecond laser pulses in lenses," *Opt. Lett.* **14**, 119–121 (1989).
19. J. Strong, *Concepts of Classical Optics* (Freeman, New York, 1958).
20. J. Paye and A. Migus, "Space-time Wigner functions and their application to the analysis of a pulse shaper," *J. Opt. Soc. Am. B* **12**, 1480–1490 (1995).